

Quantitative Gated Blood Pool Tomographic Assessment of Regional Ejection Fraction: Definition of Normal Limits

MANUEL D. CERQUEIRA, MD, FACC, GEORGE D. HARP, PhD,
JAMES L. RITCHIE, MD, FACC
Seattle, Washington

Objective. Our aim was to select a method of analysis for gated blood pool tomography that reduced variability in a group of normal subjects, allowed comparison with normal limit files and displayed results in the bull's-eye format.

Background. Abnormalities in left ventricular function may not be accurately detected by measures of global function because hyperkinesia in normal regions may compensate for abnormal regional function. Gated blood pool tomography acquires three-dimensional data and offers advantages over other noninvasive modalities for quantitative assessment of global and regional function.

Methods. Alternative methods for selecting the ventricular axis, calculating regional ejection fraction and choosing the number of ventricular divisions were studied in 15 normal volunteers to select the combination of parameter that produced the lowest variability in quantitative regional ejection fraction. Methods for quantitative comparison of regional ejection fraction with normal limit files and for display in the bull's-eye format were also examined.

Results. A fixed axis (the geometric center of the ventricle defined for end-diastole and used for end-systole) gave ejection fractions that were significantly higher in the lateral wall versus in the septum, 82 ± 6 (mean ± 1 SD) versus 39 ± 17 ($p < 0.001$) at the midcavity and 66 ± 11 versus 21 ± 20 ($p < 0.001$) at the base. A floating axis system (axis defined individually for end-diastole

and end-systole and realigned at the center) gave more uniform regional ejection fraction: 63 ± 6 versus 64 ± 8 ($p = NS$) at the midcavity and 44 ± 16 versus 45 ± 15 ($p = NS$) at the base. The coefficient of variability for regional ejection fraction was consistently lower using a floating axis. Calculating regional ejection fraction by dividing the regional stroke volume by the end-diastolic volume of the region gave a lower coefficient of variability and a more easily understood value than dividing the regional stroke volume by the total end-diastolic volume of the ventricle. Although the variability was lower using five versus nine ventricular divisions, nine regions offer greater spatial resolution. Comparison of regional ejection fraction with normal data identified regions >2.5 SD below the mean as abnormal. We described the two-dimensional bull's-eye format as a method for displaying the regional three-dimensional data and illustrated abnormalities in patients with prior myocardial infarction.

Conclusions. Gated blood pool tomography performed using a floating axis system, regional stroke volume calculation of ejection fraction and nine regions uses all the three-dimensional blood pool data to calculate regional ejection fraction, allow quantitative comparison with normal limit files, display the functional data in the two-dimensional bull's-eye format and demonstrate abnormalities in patients with myocardial infarction.

(*J Am Coll Cardiol* 1992;20:934-41)

Although indexes of global left ventricular function are important reference standards in the evaluation of heart disease, sensitive indexes of regional function are needed because patients with regional ischemia or infarction may have normal global function as a result of compensatory hyperkinesia in normal regions (1,2). Thus in a given patient, global indexes of ventricular function may lack sensitivity

for identifying abnormalities, and techniques capable of accurately assessing regional function may improve diagnostic ability.

Currently available methods for assessing regional function include contrast ventriculography (3-6), echocardiography (7-11), ultrafast computed tomography (12), nuclear magnetic resonance (NMR) imaging (13) and radionuclide techniques (14). Contrast ventriculography is an invasive two-dimensional technique that makes assumptions about ventricular geometry that may not be applicable to a ventricle distorted by infarction or ischemia. Ultrafast computed tomography and NMR imaging overcome these planar limitations but are not widely available. Echocardiography is limited by technically inadequate studies in some patients, and digital approaches to edge recognition and three-dimensional reconstruction of ventricular regions, optimal for characterization of regional function, remain in develop-

From the Division of Cardiology, Department of Medicine and the Division of Nuclear Medicine, Department of Radiology, University of Washington School of Medicine and the Department of Veterans Affairs Medical Center, Seattle, Washington. This study was supported by the General Medical Research Service of the Department of Veterans Affairs, Washington, D.C.

Manuscript received December 6, 1991; revised manuscript received March 31, 1992; accepted April 10, 1992.

Address for correspondence: Manuel D. Cerqueira, MD, Department of Veterans Affairs Medical Center (115), 1660 South Columbian Way, Seattle, Washington 98108.

mental stages. Radionuclide ventriculography can be performed in all patients, is free of geometric assumptions, is noninvasive and has a low radiation dose. Although planar methods of acquisition are limited by overlap of adjacent ventricular walls and surrounding background, gated single-photon emission computed tomographic (SPECT) imaging of the blood pool, so-called gated blood pool tomography, overcomes these limitations.

We (15,16) and others (17-19) have previously validated the accuracy of gated blood pool tomography in quantitating ventricular volumes and global ejection fraction. However, this technique has been used to assess regional function only with the use of subjective visual analysis or quantitative analysis of representative slices (17-19). A quantitative analysis technique utilizing data from the entire ventricle will improve sensitivity and allow comparison with file data on normal limits. In developing such a technique, alternative methods exist for selection of ventricular axis, calculation of regional ejection fraction and allotment of ventricular divisions. During contraction, the center of the ventricular long axis shifts between end-diastole and end-systole, and regional ejection fraction may be calculated by using a fixed method (center defined at end-diastole and used for end-systole) or floating method (axis defined and realigned at the individual end-diastolic and end-systolic centers) of axis selection. Regional ejection fraction may be calculated by dividing the stroke volume for the individual region by the total end-diastolic volume of the ventricle (the so-called global method) or by dividing the stroke volume by the volume for the region (the so-called local method). In addition, a region may be defined as a single tomographic slice or as a combination of slices.

Although regional function is heterogeneous in normal hearts (12), identification of methods that minimize variability in normal hearts should optimize identification of abnormal regional function due to disease. Thus, the purpose of our study was to 1) select the combination of gated blood pool tomographic analysis variables that gave the lowest variability in quantitative regional ejection fraction in normal human volunteers, 2) perform quantitative comparison with data from files on normal limits, and 3) display the three-dimensional data in the bull's-eye format as originally described by our group for perfusion imaging (20).

Methods

Study group. Fifteen normal male volunteers with a mean age of 33.7 ± 5 years (range 24 to 40) were studied after an overnight fast. All subjects had a <1% probability of having coronary artery disease on the basis of age, absence of cardiac risk factors and normal findings on physical examination, rest and exercise electrocardiograms (ECGs) and rest M-mode and two-dimensional echocardiograms (21). This protocol was approved by the University of Washington Human Subjects Review Committee and all subjects gave written informed consent.

Gated blood pool tomographic protocol. Acquisition. All studies were acquired with use of a 400-mm rotating gamma camera equipped with a low energy all-purpose collimator and interfaced with a dedicated computer system. After red blood cell pool labeling with 30 mCi of technetium-99m pertechnetate using a modified in vitro technique (22), each subject was placed supine on the imaging table and heart rate was sampled for 1 min to measure the mean RR interval for selecting end-systole and detecting the presence of arrhythmias. None of the subjects had arrhythmias at rest or during acquisition. We acquired the first 50 ms after the peak of the R wave for the end-diastolic frame. The 50-ms interval for the end-systolic frame was determined by using the mean RR interval and our previously described algorithm for identifying end-systole (23). Studies were acquired in a 64×64 image matrix during a 180° rotation from the left posterior oblique to the right anterior oblique position for 30 beats at each of 64 projections. Data for each beat were acquired only during end-diastole and end-systole.

Reconstruction. Each projection image was low pass filtered in the object domain by using a 5×5 spatial convolving kernel with a frequency cutoff of 0.15 cycles/projection pixel. Next, each projection was corrected for uniformity and ramp filtered in the Fourier domain. Each projection image was back-projected and simultaneously corrected for the center of rotation, and the transverse images were reconstructed. The fully reconstructed transverse images were used to define the long axis of the ventricle and oblique angle images generated in planes orthogonal to the long axis of the ventricle, as we have previously described for myocardial perfusion imaging (20).

Gated blood pool tomographic volume analysis. Left ventricular volumes were determined with visual definition of the apex and automated definition of the lateral borders and mitral valve plane (15). This technique is highly reproducible and requires only two operator interventions. First, the operator uses the summed short axis slices at end-diastole to define a generous region of interest around the left ventricle. Next, the apex is visually defined for end-diastole and end-systole on two orthogonal views as the first slice containing blood pool activity. The cavity borders are defined by an automated algorithm using a 45% threshold of the left ventricular maximal counts in each tomographic slice. Selection of the base or mitral valve plane involves calculating the stroke volume curve of each slice from the apex through the left atrium by using the region of interest described previously. The base is defined as the slice with "0" stroke volume at the mitral valve plane separating the left atrium from the left ventricle. That is, because the atrium and ventricle are beating out of phase, a slice by slice apex to left atrium stroke volume curve (using ventricular end-diastole and end-systole) will show a positive stroke volume for the ventricle, a negative stroke volume for the left atrium and "0" volume for the mitral valve plane between the atrium and ventricle. The total number of pixels/slice containing blood pool was calculated and multiplied by the pixel

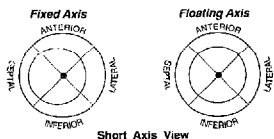


Figure 1. Fixed and floating axis systems and orientation of the ventricular regions shown in the short-axis view. For the fixed axis method, the end-diastolic geometric center is fixed in space and the end-systolic contour is superimposed on it without realignment. In the floating axis method, the center is individually defined for end-diastole and end-systole and the time-dependent motion is corrected by realignment at the centers.

volume, and individual slices were summed to obtain total ventricular volume (15).

The reconstruction, oblique angle reformatting and global volume determinations were performed once for each subject and used in all the subsequent regional analyses. This procedure minimizes variability introduced by repeated processing and allows the variability due to axis selection, method of calculating ejection fraction and number of regions to be determined independent of processing variability.

Axis selection. After the outer borders of the ventricular walls (anterior, inferior, septal and lateral, Fig. 1) were defined, the geometric center of the blood pool activity for each end-diastolic and end-systolic region of interest was identified with use of an automated algorithm. The stroke volume, end-diastolic minus end-systolic, for each region within a slice was calculated by using either a fixed or a floating axis system. The fixed axis system "fixes" in space the geometric center of the ventricular blood pool at end-diastole and superimposes on it the end-systolic contour without compensating for translation of the ventricle during contraction (Fig. 1). A floating axis system attempts to compensate for the time-dependent translation of the ventricle by realigning the end-diastolic and end-systolic frames at their center (Fig. 1). Regional ejection fractions were calculated by using the fixed and floating systems with a variable number of regions and the two methods of ejection fraction calculation to be described.

Regional ejection fraction calculation. Use of either the floating or the fixed axis selection method allowed the regional stroke volume to be calculated in each slice. The regional ejection fraction was calculated using two different methods: 1) Global = Regional stroke volume/End-diastolic volume for entire ventricle; 2) Local = Regional stroke volume/End-diastolic volume for region.

Thus, by the global method, the stroke volume for each region was divided by a single number, the total end-diastolic ventricular volume, and the local method involved division by the individual regionally calculated end-diastolic volume.

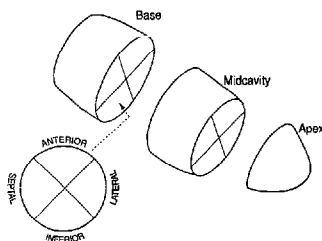


Figure 2. The left ventricular blood pool was divided perpendicular to the long axis of the heart into three equal sections. The base and midcavity were further divided into four circumferential regions corresponding to the lateral, inferior, septal and lateral walls for a total of nine regions. Combining the base and midcavity sections results in a total of five regions.

Number of regions. Although ejection fraction can be calculated for each region in each ventricular slice, we elected not to analyze or display individual slice data for several reasons. Display is more complex, variability is increased and this level of division, which exceeds the resolution limits of the tomographic system, is not accurate or clinically useful. We therefore investigated dividing the ventricle perpendicular to the long axis into either two or three apex to base sections (Fig. 2). When three sections are used, they will be referred to as apex, midcavity and base sections. The boundary slices for these three sections were defined such that each of the three sections contained approximately one third of the total slices. Divisions were made for the end-diastolic and end-systolic data sets. The midcavity and base sections were further divided into 90° circumferential regions that correspond to the lateral, inferior, septal and anterior ventricular walls and gave a total of nine ventricular regions. The midcavity and base sections also were summed to create a single base section consisting of two thirds of the entire blood pool and having four regions corresponding to the lateral, inferior, septal and anterior ventricular walls. With the apex this procedure resulted in a total of five regions.

Quantitative analysis and display. The mean and standard deviation of the ejection fraction for each region were calculated in the 15 normal subjects by using the various combinations of axis selection, method of ejection fraction calculation and number of regions. These values established the limits of normal for regional ejection fraction. Each of the 15 subjects was then compared with the composite normal file to determine the range of variability and the lower limits of standard deviations that correctly identified each individual as having a normal regional ejection fraction.

Statistics. All data are expressed as the mean value \pm 1 SD in the text and diagrams and as the mean value \pm 1 SEM

Table 1. Effects of Axis Selection and Method of Calculation on Regional Ejection Fraction in Normal Subjects

	Local Method			Global Method		
	Fixed	Floating	p Value	Fixed	Floating	p Value
Apex	66 ± 8	66 ± 8	NS	13.5 ± 2.6	13.5 ± 2.6	NS
Midcavity						
Lateral	82 ± 8	64 ± 8	<0.0001	6.1 ± 0.9	5.8 ± 1.1	<0.0001
Inferior	68 ± 9	68 ± 7	NS	7.0 ± 1.1	7.0 ± 1.2	NS
Septal	39 ± 17	63 ± 6	<0.0001	3.4 ± 1.6	5.3 ± 0.9	<0.0001
Anterior	72 ± 9	67 ± 6	NS	7.9 ± 1.2	7.3 ± 0.9	NS
Base						
Lateral	66 ± 11	45 ± 15	<0.0001	5.5 ± 1.5	3.8 ± 1.6	<0.0001
Inferior	54 ± 15	52 ± 7	NS	6.2 ± 2.4	5.9 ± 1.4	NS
Septal	20 ± 21	44 ± 16	<0.0001	1.9 ± 2.0	4.2 ± 1.8	<0.0001
Anterior	55 ± 11	52 ± 13	NS	6.8 ± 1.7	6.6 ± 2.3	NS
Total base						
Lateral	74 ± 8	54 ± 10	<0.0001	11.7 ± 2.0	8.6 ± 2.1	<0.0001
Inferior	61 ± 10	60 ± 4	NS	13.3 ± 2.6	12.9 ± 1.3	NS
Septal	29 ± 11	53 ± 9	<0.0001	5.2 ± 2.0	9.4 ± 1.8	<0.0001
Anterior	63 ± 7	59 ± 7	NS	14.8 ± 1.8	14.0 ± 2.2	NS

In the fixed method of calculating ejection fraction, the center of the ventricular long axis is defined at end-diastole and used for end-systole; in the floating method the axis is defined and realigned at individual end-diastolic and end-systolic centers. In the global method the stroke volume for the individual region is divided by the total end-diastolic volume of the ventricle; in the local method it is divided by the volume for the region.

in graphs. The coefficient of variability in each region using all 15 subjects was calculated as: Coefficient of variability = (SD/Mean) × 100. Comparisons between methods were performed using a two-tailed Student *t* test for paired data and the Bonferroni correction applied to correct for performing multiple comparisons. A *p* value ≤ 0.0005 was considered significant.

Results

Apex to base variation in regional ejection fraction. Table 1 shows the regional ejection fraction at the apex, midcavity, base and total base sections obtained by using the fixed or floating axis and local or global methods of ejection fraction calculation. The apical ejection fraction was not changed by axis selection or by the number of base divisions. For both the floating and the fixed axis method, ejection fraction was 66 ± 8% (range 54% to 82%) with a coefficient of variability of 13% for local and 13.5 ± 2.6% (range 10.3% to 17.8%) with a coefficient of variability of 19% for global methods. The ejection fraction for a given section (mean of the four regions in the midcavity or base) was the same for the fixed and floating axis systems with either the local or the global method: 66% and 6.1% for the midcavity and 48% and 5.1% for the base.

Effect of axis selection. Figure 3 shows the effect of axis selection on regional ejection fraction at the midcavity and base level obtained with the local method of calculation. In the midcavity with use of a fixed axis, the mean septal ejection fraction is 39 ± 17% (range 2% to 64%) and the mean lateral ejection fraction is 82 ± 8% (range 65% to 94%). With use of a floating axis, septal ejection fraction increases to 63 ± 6% (range 53% to 74%) and lateral ejection fraction

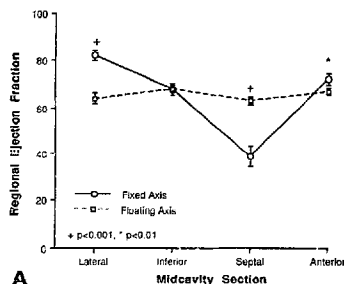
decreases to 64 ± 8% (range 49% to 79%) relative to the comparable areas measured with the fixed method. These differences were highly significant (*p* < 0.0001). The regional ejection fraction changes resulting from axis system selection in the anterior and inferior regions were smaller and not statistically significant.

Ejection fraction for the base regions was lower than that of the matching midcavity regions for both axis systems. A similar pattern of low septal (21 ± 20%, range 34% to 49%) and high lateral (66 ± 11%, range 47% to 84%) ejection fractions was found by using the fixed axis. With the floating axis, septal ejection fraction increased and the lateral ejection fraction decreased (*p* < 0.001) without significantly altering the values for the inferior and anterior segments.

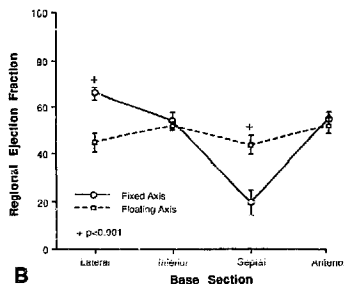
These same axis system relations for regional ejection fraction were found for the midcavity and base sections by using the global method of calculation and are shown in Figure 4.

Figure 5 compares the mean sectional coefficient of variability, the average of the four regions within a section, at the midcavity and base, for the fixed and floating axis and global and local methods of ejection fraction calculation. The coefficient of variability shows three distinct trends: 1) it is largest in the base, 2) it is largest with the global method, and 3) it is largest with a fixed axis system.

Effects of ejection fraction calculation methods. Regional ejection fraction calculated with the global method (dividing the stroke volume for each region by the total ventricular volume) is shown in Table 1 and Figure 4. This method resulted in very low regional ejection fraction values that do not convey the range of normal that we have come to associate with the total ventricular ejection fraction, and for this reason the local method is more easily understood. The



A



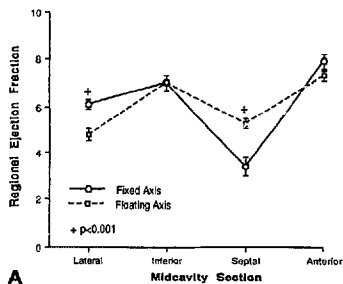
B

Figure 3. Regional ejection fraction (mean \pm SEM) in 15 normal subjects obtained with the local method is plotted at the midcavity (A) and base (B) levels for the lateral, inferior, septal and anterior walls for the use of the fixed and floating axis systems. The floating system produces a more uniform circumferential distribution of regional ejection fraction.

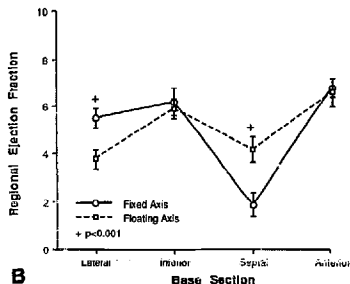
global method also produced greater variability in normal values as reflected by the higher coefficient of variability for all regional comparisons (Fig. 5).

Effects of number of regions. When the midcavity and base sections were combined to give a total base section or five regions (Table 1), the relations for normalization and method of axis selection were similar to those described earlier. However, the standard deviations and coefficient of variability are lower, suggesting a lesser degree of variability and more homogeneous regional ejection fractions when larger regions are used.

Definition of normal limits. After regional ejection fraction means and standard deviations were generated for all possible combinations of the aforementioned variables in the 15 normal subjects, each region in each subject was compared with the group mean and the number of standard



A



B

Figure 4. Regional ejection fraction (mean \pm SEM) in 15 normal subjects obtained with the global method is plotted at the midcavity (A) and base (B) levels for the lateral, inferior, septal and anterior walls with use of the fixed and floating axis systems. Similar to the local method, the floating system produces a more uniform sectional distribution of regional ejection fraction.

deviations above or below the group mean was determined. The lowest number of standard deviations below the mean in any region for any subject was -2.8 with the global method and -2.5 with the local method of calculating ejection fraction.

Display of three-dimensional ejection fraction data. We have previously described a technique (bull's-eye) for displaying the three-dimensional perfusion data acquired by SPECT thallium-201 imaging (20). This method not only allows the actual three-dimensional data to be displayed in a two-dimensional format but facilitates the display of a quantitative comparison to normal limits. The bull's-eye format in Figure 6 displays data in the angiographic left anterior oblique view, such that major coronary artery beds are easily distinguished: the septal and anterior walls supplied by the left anterior descending coronary artery are on the left

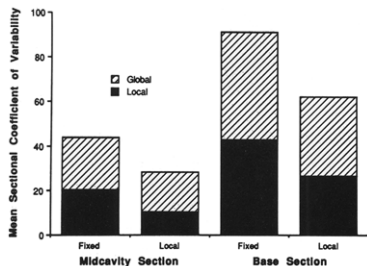
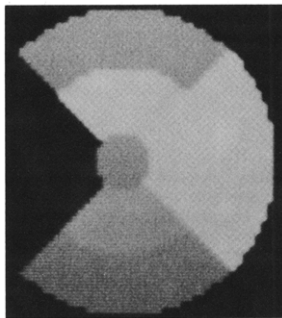


Figure 5. Mean sectional coefficient of variability. This value is greatest for the global method, in the base as opposed to the midcavity section, and with use of the fixed axis system. Each bar represents the mean coefficient of variability in all 15 patients of the four circumferential regions in a section.

and at the top; the inferior wall supplied by the posterior descending coronary artery is at the bottom, and the lateral wall supplied by the left circumflex artery is to the right. The apex is shown as the center of the bull's-eye, the midcavity is the middle ring and the base is the outermost ring. Each segment keeps the same orientation as described above. This format allows the regional topographic variability in ejection fraction to be appreciated.

Figure 6. Quantitative gated blood pool tomographic regional ejection fraction bull's-eye display in a patient with two prior myocardial infarctions. Analysis used a floating axis system, local ejection fraction calculation and nine ventricular regions. See text for orientation. Regional ejection fraction is markedly abnormal in the septum (black), abnormal in the base and midcavity of the inferior wall, apex and base of the anterior wall (gray). The basal and midcavity portions of the lateral wall and the midcavity portion of the anterior wall are normal (white).



Regional ejection fractions were calculated by using a floating axis system with local normalization in a patient with prior myocardial infarctions in the territory of the right and left anterior descending arteries (Fig. 6). Each of the nine regional ejection fractions was compared with normal limits established from the 15 young healthy subjects. All regions ± 2.5 SDs are displayed as white and all regions < -2.5 SD are shown on a gray scale with black representing the lowest value.

With use of this bull's-eye method of display, comparisons can be made between perfusion, measured at rest with thallium, and ventricular function. Figure 7 shows data from a patient with a lateral wall myocardial infarction. Regional ejection fractions, measured by quantitative gated blood pool tomography and compared with data in normal limit files, are abnormal in the regions with thallium-201 abnormalities. The greater size of the thallium-201 perfusion defect reflects, in part, the difference in resolution between the thallium and gated blood pool tomographic methods.

Discussion

Our results demonstrate the feasibility of using the three-dimensional data from gated blood pool tomography to quantitative regional ejection fraction, perform quantitative comparisons with normal limits, display the three-dimensional data in the two-dimensional bull's-eye format and demonstrate abnormalities in patients with myocardial infarction.

Fixed versus floating axis frame of reference. The use of a floating axis system with the local method of ejection fraction calculation produced the lowest degree of variability in normal hearts and should be optimal for demonstrating regional abnormalities in diseased hearts. In 15 normal subjects, we found that the fixed axis system resulted in greater regional ejection fraction heterogeneity; ejection fraction was low in the septum and high in the lateral wall region. Because the normal subjects had a low probability of any form of heart disease and no prior infarction, we believe that this heterogeneity in ejection fraction derives, in part, from the method of analysis. That is, during contraction, the cardiac long axis translates toward the septum, producing a low ejection fraction if this translation is not corrected. When a floating axis system is employed, the ejection fraction in the lateral and septal segments is more uniform (24,25). Potel et al. (25) studied the three-dimensional motion of coronary artery bifurcations in humans using biplane coronary arteriograms. Using computer modeling techniques, they concluded that a moving or floating axis system gave the best representation of wall motion. In patients with visually defined regional abnormalities, this method was the most promising for correctly identifying such regions. Similar findings (7) of reduced regional heterogeneity obtained with the floating axis system have been reported for two-dimensional echocardiographic analysis of regional wall motion. Ultrafast computed tomographic analysis is routinely

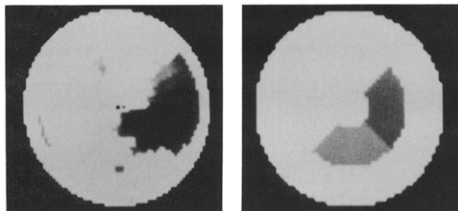


Figure 7. Bull's-eye displays. *Left.* The quantitative thallium-201 perfusion defect. *Right.* The quantitative gated blood pool tomographic regional ejection fraction. Regional ejection fraction for nine regions was calculated using the local method and a floating frame of reference axis system. Both perfusion and ejection fraction are abnormal in the midcavity portion of the inferior and lateral walls.

performed by using a floating axis system to minimize variability (12). Because all the data obtained with gated blood pool tomography are both digital and three-dimensional, realignment along a geometrically appropriate axis can be and is accomplished in an automated fashion. This approach has not been implemented in contrast ventriculography and is rarely performed for echocardiography.

Number of ventricular regions. Variability was lower when five as opposed to nine ventricular regions were used. This was true for both methods of ejection fraction calculation and axis systems. However, nine regions provide better spatial resolution and may be more sensitive for detection of regional differences in a given patient or populations. This hypothesis remains to be proved.

Bull's-eye display. The absolute three-dimensional regional ejection fraction values from gated blood pool tomography can be displayed easily in the two-dimensional bull's-eye format (Fig. 6 and 7). This format facilitates assimilation of the three-dimensional functional data with an appreciation of the topography relative to the coronary anatomy. Alternative visual display methods have been proposed (26). Our method allows quantitative comparison with normal limits and provides a format for displaying the results. Pilot studies in patients with known myocardial infarction have shown good agreement between the tomographically localized quantitative thallium-201 perfusion defect and the quantitative gated blood pool tomographically defined regional ejection fraction abnormalities.

Comparison with other gated blood pool tomographic methods. Other published gated blood pool tomography methods (17,19) of regional analysis have relied on calculating regional ejection fraction from a representative mid-cavity long-axis slice and using a centerline method similar to that used to analyze contrast ventriculograms. These methods measure the fractional shortening between end-diastole and end-systole for a region and divide this change by the end-diastolic length. These methods do not use all the three-dimensional volume data available from the acquisition. A second method of gated blood pool tomographic regional analysis also has been reported that relies on cord changes from all the three-dimensional data but does not readily allow quantitative comparison (27). Our method of

quantitative regional analysis uses the entire three-dimensional volume data rather than selected slices, and the results accurately reflect regional function of the entire ventricle.

Comparison with contrast ventriculography and echocardiography. The centerline method for contrast ventriculographic analysis of regional function normalizes the fractional shortening for each cord by dividing a given cord by the total ventricular end-diastolic perimeter length rather than by the end-diastolic length for the specific cord (3-5). This method of normalization decreases the variability of motion in normal subjects, improves the ability to detect abnormal function in patients with prior myocardial infarction and compensates for differences in absolute ventricular volumes (3). A similar centerline method using the end-diastolic perimeter has been developed for echocardiography, but methods using either hemiaxis length, perimeter length or the diastolic area for the local region also are used (7,8). This method of normalization is similar to the global method of ejection fraction calculation used in our study, but it had a higher coefficient of variability and the very low ejection fraction values are difficult to understand. A limitation of contrast ventriculography and echocardiography is that analysis is performed on single or biplane studies or selected slices and not routinely performed for the entire ventricle. This geometric limitation results in sampling bias and the three-dimensional information recorded by tomographic methods is theoretically more accurate.

Ultrafast computed tomography and nuclear magnetic resonance imaging. Ultrafast computed tomography acquires three-dimensional data and is capable of generating regional ejection fractions, but this technique is not widely available, requires contrast injections and is technically demanding (12). Nuclear magnetic resonance imaging has the potential to accurately assess regional function, but studies reported to date (13) have relied on visual analysis of representative slices.

Clinical implications. These results show that although there is heterogeneity in regional ejection fraction in normal hearts when measured by gated blood pool tomography, regional function can be well characterized and methods of analysis selected to minimize the variability. Our technique

of gated blood pool tomographic regional ejection fraction analysis avoids the limitations of planar methods of acquisition and the sampling bias introduced by the use of representative ventricular slices in echocardiography and other gated blood pool tomography methods of analysis. Prospective evaluation of this approach in patients with myocardial infarction is needed to determine sensitivity. Gamma cameras capable of performing gated blood pool tomography exist in most nuclear medicine departments and this technique should be readily available in most hospitals. The quantitative measurement of regional ejection fraction allows display in the bull's-eye format, and comparisons with files on normal limits can be readily performed. The time required for acquisition of gated blood pool tomography currently precludes studies during exercise stress. Another potential application of this method is gated acquisition of technetium-labeled isonitrites, which may allow evaluation of regional wall thickening.

Limitations. Our technique acquired only the end-diastolic and end-systolic portions of the heart cycle and did not perform arrhythmia rejection. If arrhythmias or marked changes in heart rate occur during acquisition, the end-systolic period of minimal volume may be distorted and this distortion will introduce errors in both global and regional ejection fraction. Because we documented the absence of arrhythmias or changes in heart rate during the acquisition in our normal subjects, our results should not have been affected by such changes. However, if this technique is to be used in patients with arrhythmias, careful monitoring or the use of an algorithm to perform arrhythmia rejection is recommended. Such algorithms are commercially available. The greater variability observed at the base of the heart may be due to errors in accurately identifying the mitral valve plane or transecting it at an angle. Our automated phase base selection method minimizes user intervention and is highly reproducible, but visual inspection and modification are recommended (15,20).

References

1. Studius M, Maynard C, Fritz J, et al. Coronary anatomy and left ventricular function in the first 12 hours of acute myocardial infarction: the Western Washington Randomized Intracoronary Streptokinase Trial. *Circulation* 1985;72:792-797.
2. Martin G, Sheehan F, Studius M, et al. Intravenous streptokinase for acute myocardial infarction: effects on global and regional systolic function. *Circulation* 1989;79:258-266.
3. Sheehan F, Stewart D, Dodge H. Variability in the measurement of regional left ventricular wall motion from contrast angiograms. *Circulation* 1983;67:550-9.
4. Sheehan F, Bolton E, Dodge H, Mathey D, Schofer J, Woo H-W. Advantages and applications of the centerline method for characterizing regional ventricular function. *Circulation* 1986;74:293-305.
5. Sheehan F, Schofer J, Mathey D. Measurement of regional wall motion from biphasic contrast ventriculograms: a comparison of the 30 degree right anterior oblique and 60 degree left anterior oblique projections in patients with acute myocardial infarction. *Circulation* 1986;74: 96-104.
6. Goodyer A, Langou R. The multicentric character of normal left ventricular wall motion. Implications for the evaluation of regional wall motion abnormalities by contrast angiography. *Cathet Cardiovasc Diagn* 1982;8: 225-32.
7. Moyimhan P, Parisi A, Feldman C. Quantitative detection of regional left ventricular contraction abnormalities by two-dimensional echocardiography. I: analysis of methods. *Circulation* 1981;63: 4753-60.
8. Moyimhan P, Parisi A, Feldman C. Quantitative detection of regional left ventricular contraction abnormalities by two-dimensional echocardiography. II: accuracy in coronary artery disease. *Circulation* 1981;63:752-60.
9. Wohlgeleitner D, Jaffe C, Cabin H, Yeatman L, Cleman M. Silent ischemia during coronary occlusion produced by balloon inflation: relation to regional myocardial dysfunction. *J Am Coll Cardiol* 1987;10:491-8.
10. Pearlman J, Hogan R, Wiske P, Franklin T, Weyman A. Echocardiographic definition of left ventricular centroid. I. Analysis of methods for centroid calculation from a single tomogram. *J Am Coll Cardiol* 1990;16: 986-92.
11. Wiske P, Pearlman J, Hogan R, Franklin T, Weyman A. Echocardiographic definition of the left ventricular centroid. II. Determination of the optimal centroid during systole in normal and infarcted hearts. *J Am Coll Cardiol* 1990;16:993-9.
12. Ferrag A, Rumberger J, Reiter S, et al. Sectional segmental variability of left ventricular function: experimental and clinical studies using ultrafast computed tomography. *J Am Coll Cardiol* 1988;12:415-23.
13. Lutan C, Cranney G, Bouchard A, Bittner V, Pohost G. The value of cine nuclear magnetic resonance imaging for assessing regional ventricular function. *J Am Coll Cardiol* 1989;14:1721-9.
14. Sturling M, Walsh R, Lasher J, Lancaster J, Blumhardt R. Quantification of left-ventricular regional dysynergy by radionuclide angiography. *J Nucl Med* 1987;28:1725-35.
15. Studius M, Williams D, Harp G, et al. Left ventricular volume determination using single-photon emission computed tomography. *Am J Cardiol* 1985;55:1185-91.
16. Studius M, Ritchie J. Gated blood pool tomography. In: Pohost GM, Morganroth J, Ritchie J, eds. *New Concepts in Cardiac Imaging*. Chicago: Year Book Medical Publishers, 1986:137-54.
17. Barnat J-L, Brendel A, Colle J-P, et al. Quantitative analysis of left-ventricular function using gated single photon emission tomography. *J Nucl Med* 1984;25:1167-74.
18. Corbett J, Jansen D, Lewis S, et al. Tomographic gated blood pool radionuclide ventriculography: analysis of wall motion and left ventricular volumes in patients with coronary artery disease. *J Am Coll Cardiol* 1985;6:349-58.
19. Gill J, Moore R, Tamaki N, et al. Multigated blood-pool tomography: a new method for the assessment of left ventricular function. *J Nucl Med* 1986;27:1916-24.
20. Caldwell J, Williams D, Harp G, Stratton J, Ritchie J. Quantitation of size of relative myocardial perfusion defect by single photon-emission computed tomography. *Circulation* 1984;70:19-8-56.
21. Diamond G, Forrester J. Analysis of probability as an aid in the clinical diagnosis of coronary-artery disease. *N Engl J Med* 1979;300:1350-8.
22. Calahan R, Froelich J, McKusick K, Leppo J, Strauss H. A modified method for the in vivo labeling of red blood cells with Tc-99m: coactive communication. *J Nucl Med* 1982;23:315-8.
23. Graham M, Cavallifles F, Ritchie J, et al. Performance characteristics of a commercial ECG gate. *J Nucl Med* 1980;21:387-90.
24. Clayton P, Jeppson G, Klauuser S. Should a fixed external reference system be used to analyze left ventricular wall motion? *Circulation* 1982;7:1518-21.
25. Patel M, MacKay S, Rubin J, Assen A, Sayre R. Three dimensional left ventricular wall motion in man: coordinate systems for representing wall movement direction. *Invest Radiol* 1984;19:497-509.
26. Miller T, Wallis J, Sampathkumaran K. Three-dimensional display of gated cardiac blood-pool studies. *J Nucl Med* 1989;30:2036-41.
27. Faber T, Stokely E, Templeton G, Akers M, Parkey R, Corbett J. Quantification of three-dimensional left ventricular regional wall motion and volumes from gated tomographic radionuclide ventriculograms. *J Nucl Med* 1989;30:638-49.